LBL-27783
Preprint

Lawrence Berkeley Laboratory
UNIVERSITY OF CALIFORNIA

Submitted to Physics Letters B

Antiproton Production as a Baryonometer in Ultrarelativistic Heavy Ion Collisions

S. Gavin, M. Gyulassy, M. Plümer, and R. Venugopalan

October 1989

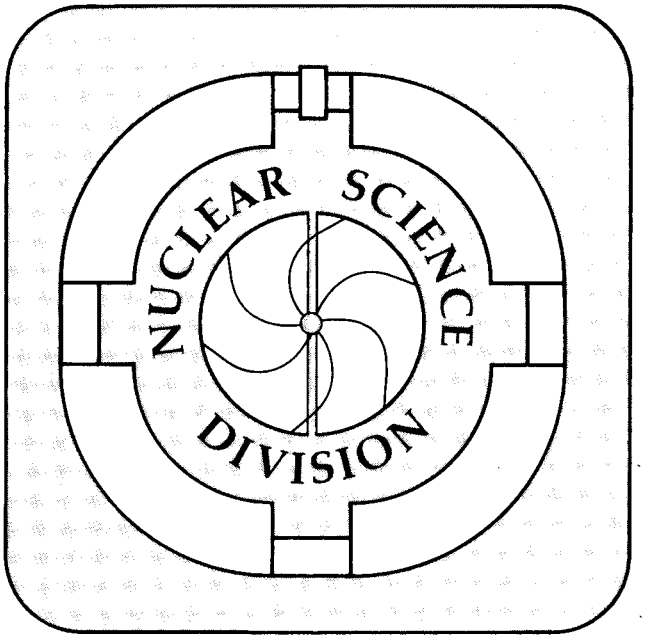

Prepared for the U.S. Department of Energy under Contract Number DE-AC03-76SF00098.

DISCLAIMER

LBL-27783

Antiproton Production as a Baryonometer in Ultrarelativistic Heavy Ion Collisions*

S. Gavin,[a] M. Gyulassy, M. Plümer,[b] and R. Venugopalan[c]

Nuclear Science Division
Mailstop 70A-3307
Lawrence Berkeley Lab
Berkeley, CA 94720 USA

Abstract:
We propose that measurements of the antiproton and proton yields in ultrarelativistic nucleus-nucleus collisions can provide a sensitive probe of the spacetime evolution in these reactions. We estimate the antiproton suppression expected due to annihilation processes for collisions in the energy range $\sqrt{s} = 10 - 200$ AGeV.

* This work was supported by the Director, Office of Energy Research, Division of Nuclear Physics of the Office of High Energy and Nuclear Physics of the U.S. Department of Energy under Contract No. DE-AC03-76SF00098.

[a] Present address: Research Institute for Theoretical Physics, Siltavuorenpenger 20 C, 00170 Helsinki, Finland.

[b] Postdoctoral Fellow of Deutsche Forschungsgemeinschaft.

[c] Permanent address: Physics Dept., SUNY at Stony Brook, Stony Brook, NY, 11794

Experiments with ultrarelativistic nuclear beams on heavy targets offer the opportunity for studying matter at extreme energy and baryon densities [1]. While the suppression of J/ψ production strongly supports the expectation that matter at energy densities > 1 GeV/fm^3 is produced [1,2], there is little direct information on the baryon density as yet. Global features of the data such as the transverse energy and rapidity distributions are comparably described by a variety of dynamical scenarios from string models [3,4,5,6], which describe the nucleus-nucleus collision as a superposition of nucleon-nucleon subcollisions, to hydrodynamic models, which incorporate a high degree of collectivity [7]. These models differ dramatically in the spacetime evolution of the leading baryons. In the string picture, particle formation occurs subsequent to the individual NN subcollisions, so that high-baryon-density matter is never realized in the central region. An opposite extreme is the Landau hydrodynamic model, where the baryons are fleetingly 'stopped' in a high-density fireball and then swept to high rapidities by shocks.

In this paper we suggest that antiproton suppression is a sensitive probe of the spacetime evolution of baryons in heavy-ion collisions. Specifically, we expect that the antiproton-to-proton ratio is suppressed relative to that found in nucleon-nucleon reactions due to antibaryon annihilation with comoving baryons. We derive a simple expression for the relative yield in central collisions,

$$R \equiv \frac{dN_{\overline{p}}/dy}{dN_p/dy} \approx R_0 \left(\frac{t_0}{t_F}\right)^{\beta}, \tag{1}$$

in terms of the proper antiproton-formation time, t_0, and the average freezeout proper time t_F. The absorption parameter,

$$\beta \approx \frac{\langle \sigma_a v \rangle}{\pi {R_A}^2} \frac{dN_B}{dy}, \tag{2}$$

depends on the well-known $p\overline{p}$ annihilation cross section, the baryonic-charge rapidity density dN_B/dy, and the projectile radius $R_A \approx 1.2\, A^{1/3}$ fm. The ratio (1) is analogous to the survival probability of a J/ψ in a dense hadron gas — the essential difference is that the absorption parameter in the J/ψ case depends on the total rapidity density of hadrons [8], while (2) depends on the net baryon density. The initial antibaryon concentration

$$R_0 \equiv \overline{n}(t_0)/n(t_0) \tag{3}$$

is the ratio of the densities of antibaryons and baryons in the central region in configuration space. We expect R_0 to be roughly the $\overline{p}$ to p measured in pp collisions.

Measurements of $\overline{p}$ and p production can be used to extract information on spacetime evolution in two alternative ways:

1. The ratio can be used as a *chronometer* for measuring the ratio of the freezeout time t_F to the formation time t_0.

2. The ratio can be used as a *baryonometer* to measure the initial densities of baryons and antibaryons.

In the first capacity, $\overline{p}$ and p data can provide information on the spacetime evolution of the collision complementary to that on t_f and t_0 from pion interferometry [9] and lepton-nucleus data respectively [10]. However, for this the initial ratio R_0 must be taken from pp data or from some dynamical model. In the second role, we can determine the initial densities of baryons and antibaryons in order to gain insight on the formation mechanism, provided we have supplementary information on the global evolution, e.g., from interferometry data. Novel effects such as quark-gluon-plasma production [11] and color-rope formation [12] and chiral fluctuations (A. Mueller in [1]) can cause the initial baryon concentration to differ from the pp value. As a baryonometer, the probe is therefore sensitive to the collectivity associated with high densities in the collision.

Experimental information on the baryon rapidity distributions at CERN and BNL is not currently available, although work is in progress [13]. We combine a final-state interaction model incorporating scaling dynamics [14] with the LUND string model to exhibit these complementary roles of $\overline{p}$ and p measurements. The rapidity distributions rapidity distributions expected in the absence of annihilation, based on the ATTILA [4] version of the LUND/Fritiof model [3], are shown in Fig. 1. Below, we shall use these distributions to illustrate the magnitude of the suppression effect due to annihilation. Antibaryons can be annihilated in collisions with comoving secondary baryons and 'stopped' valence baryons. The final antiprotons are formed both directly and through the decay of more massive antibaryons such as $\overline{\Delta}$'s and $\overline{\Lambda}$'s. Annihilation can proceed through a variety of channels, such as $\overline{N}N$, $\overline{\Delta}N$, and $\overline{N}\Lambda$. The $N\overline{N}$ annihilation cross section is large, ~ 40 mb [15], at the energies typical of interactions between comovers. Annihilation by comoving, i.e., similar-rapidity, baryons is dominant, since the annihilation cross section falls off with increasing energy.

In order to study the antibaryon evolution in the presence of baryons, we apply a hadrochemistry approach similar to that used by B. Friman in Ref. [1]. Annihilation reduces the density of comoving antibaryons at the rate

$$(d\overline{n}/dt)_a = -\langle\sigma_a v\rangle n\overline{n} = -\langle\sigma_a v\rangle(n_B + \overline{n})\overline{n}, \tag{4}$$

where n and $\overline{n}$ are the densities of baryons and antibaryons, and $n_B = n - \overline{n}$ is the baryonic-charge density. The rate coefficient $\langle\sigma_a v\rangle$ is given by

$$\langle\sigma_a v\rangle = \frac{1}{n\overline{n}} \sum_{b,\overline{b}} \int \frac{d\Gamma_b}{E_b} \frac{d\Gamma_{\overline{b}}}{E_{\overline{b}}} f_b f_{\overline{b}} \sigma_a^{b\overline{b}}(s) F_{b\overline{b}}(s) \tag{5}$$

where f_b and $f_{\overline{b}}$ are the phase-space distributions for baryon and antibaryon species b and $\overline{b}$, and $F_{b\overline{b}}(s) = \{(s - (m_b + m_{\overline{b}})^2)(s - (m_b - m_{\overline{b}})^2)\}^{1/2}/2$ is an invariant flux factor. We neglect Pauli blocking in (5), since the phase-space density of each baryon species is $\ll 1$. The density of baryons of species b is $n_b = \int d\Gamma_b\, f_b(E_b)$ for

$d\Gamma_b \equiv g_b d^3p_b/(2\pi)^3$, $E_b = \sqrt{{p_b}^2 + {m_b}^2}$, and g_b the number of spin degrees of freedom. Note that a similar formulation has been used in [16] and [17] in the problem of subthreshold antiproton production.

To estimate $\langle \sigma_a v \rangle$, we assume that $N\overline{N}$ annihilation is typical of the many channels that contribute to (5), so that $\langle \sigma_a v \rangle \approx \langle \sigma_a^{N\overline{N}} v \rangle$, and take a Boltzmann-like phase-space distribution $f_b(E) \propto \mathrm{e}^{-E/T_b}$. The slope parameter $T_b = 160$ MeV is fixed such that $\langle p_\perp \rangle \approx 0.6$ GeV for baryons. Using the parametrization of $p\overline{p}$ annihilation data [15] of Koch and Dover [17], we find

$$\langle \sigma_a v \rangle \approx \langle \sigma_a^{p\overline{p}} v \rangle \approx 40 \text{ mb}. \tag{6}$$

This result, however, changes by less than 1% for T_b in the range from 100 to 200 MeV. Furthermore, the integrals in (5) are very insensitive to m_b.

In the longitudinally expanding system, the density of antibaryons satisfies

$$d\overline{n}/dt + \overline{n}/t \equiv (d\overline{n}/dt)_a = -\langle \sigma_a v \rangle (n_B + \overline{n})\overline{n}, \tag{7}$$

where we assume that the four velocity of the flow has roughly the scaling form $v^\mu \approx (t^2 - z^2)^{-1/2}(t, 0, 0, z)$ [14]. Similarly, baryonic-charge conservation implies $dn_B/dt + n_B/t = 0$, so that $n_B = n_B(t_0)t_0/t$. If the evolution is dominated by the longitudinal expansion from formation at t_0 to freezeout at t_F, then the baryonic-charge rapidity density

$$dN_B/dy = \pi {R_A}^2 n_B(t_F) t_F = \pi {R_A}^2 n_B(t_0) t_0 \tag{8}$$

is time independent. We solve (4) and find that the rapidity density of antibaryons satisfies

$$\frac{d\overline{N}/dy|_{t_F}}{dN_B/dy} = \frac{d\overline{N}/dy|_{t_0}}{dN/dy|_{t_0}\,(t_F/t_0)^\beta - d\overline{N}/dy|_{t_0}} = \frac{R}{1-R} \tag{9}$$

where R is the antiproton-to-proton ratio (1). Eqs. (8) and (9) are applicable in both the hydrodynamic and the kinetic regimes up to the time when transverse expansion becomes important. We assume that freezeout of the baryon-chemistry occurs roughly at the time that the flow becomes three-dimensional, $t_F \sim R_A/v_S$, where $v_S \sim 1/\sqrt{3}$ is the sound velocity, since the rate term $(d\overline{n}/dt)_a$ is much smaller than the drift term $\overline{n}/t$. The formation time is expected to vary between 2 – 1 fm at $\sqrt{s} = 20$ GeV to 200 GeV.

As noted above, the ratio (9) together with measurements of dN_p/dy and $dN_{\overline{p}}/dy$ can be used to determine the ratio t_F/t_0, if the initial ratio R_0 is extrapolated from pp data, or calculated within a specific model. In Fig. 2 we show the final $dN_{\overline{p}}/dy$ for S + Au and Au + Au at 200 AGeV for various values of t_F/t_0. The curve for $t_0 = t_F$ is the initial rapidity density calculated using ATTILA and the other curves are obtained using (9). We see that the suppression of antiproton production can be considerable depending on the value of t_F/t_0. The suppression for other systems and energies for $y = 0$ are compiled in Table 1 (note that the baryon and antibaryon

rapidity densities, dN/dy and $d\overline{N}/dy$, in Table 1 include all baryonic species — as opposed to Fig. 2, where the $\overline{p}$ distributions are presented).

Alternatively, we can extract information on the initial rapidity densities from data, provided that we know t_F/t_0 from a dynamical model or from other experiments. For the reaction Au+Au, Fig. 3 illustrates how such information can be obtained from the correlation between the measured antiproton yield and the proton contribution to the baryonic-charge rapidity density. The curves correspond to fixed values of the *initial* scalar baryon rapidity density, $dN_S/dy \equiv dN/dy + d\overline{N}/dy$, a quantity which reflects the degree of excitation of the system. The correlation is essentially independent of the beam energy and varies slowly with the projectile and target type through the derived dependence on t_F/t_0 (cf. eqs.(1), (9)). The expected correlations for the initial conditions taken from Fig. 1 are shown in Fig. 3 as "data" points. A complex behavior of the scalar density expected from LUND for increasing energy is revealed — we see that the initial dN_S/dy is relatively high at the lowest energy simply because the density of baryons is high due to stopping. The scalar density drops as transparency becomes more pronounced (cf. Fig. 1) but rises again at RHIC due to the enhanced production of baryon-antibaryon pairs.

The full hadrochemistry problem involves back reaction processes that could produce antibaryons through a variety of reactions in a high density hadron gas, $\pi\pi \rightarrow N\overline{N}$, $\rho\rho \rightarrow N\overline{N}$, etc. We expect that the contribution of these channels to antibaryon production will be small, however, since the channels that involve the most abundant mesons are endothermic — the π, K, η, ρ, ω, K^* and η' which constitute $\sim 90\%$ of the secondaries in LUND have masses of less than 1 GeV so that the reactions are threshold suppressed. To illustrate the effect of possible inverse processes on the yield, we take the $\rho\rho$ channel to be dominant. For nuclear collisions at Bevalac energies, Ko and Ge [16] pointed out that the $\rho\rho$ channel can be strong, since the ρ is massive and $p\overline{p} \rightarrow \rho\rho$ has a relatively large branching ratio - they estimate $\sim 5\%$. Moreover, ρ's are plentiful at CERN energies, accounting for $\sim 20\%$ of the secondaries. We add the source term $\langle\sigma_s v\rangle {n_\rho}^2$ to (4), where n_ρ is the ρ density. Applying detailed balance to $p\overline{p}$ annihilation data as in Ref.[16], we find that $\langle\sigma_s v\rangle \approx \langle\sigma_{\rho^+\rho^-} v\rangle \approx 0.2\,\mathrm{mb}$ for an effective temperature $T_\rho \approx 160$ MeV, as characterizes the transverse momentum distribution in LUND. To obtain the upper bounds for the final rapidity densities of baryons and antibaryons in Table 1, we assumed that dN_ρ/dy is time-independent and given by the values shown in Fig. 1 . The modified rate equation then determines the upper bounds in Table 1; the lower bounds correspond to the absence of a ρ contribution. The conserved-ρ approximation overestimates the effect of antibaryon regeneration by overemphasizing the effect of the strongest channel, since ρ decay is neglected.

Finally, we briefly comment on antibaryon production at AGS energies. At these energies we expect the nuclei to be fully stopped (see Fig. 1), so that Landau hydrodynamics may be more appropriate than our scaling approximation. Furthermore, our simplified treatment of freezeout is not applicable because t_F is on the order of the spread in the formation time t_0 and a much more detailed dynamical

calculation is necessary. Our simplified treatment applies only in the scaling regime.

We are grateful to J. Costales, B. Jacak, and J. Kapusta for valuable discussions. This work was supported in part by the Director, Office of High Energy and Nuclear Physics of the Department of High Energy and Nuclear Physics of the Department of Energy under contracts DE-AC02-76ER13001 and DE-AC03-76SF00098.

References

[1] G. Baym, P. Braun-Munziger, and S. Nagamiya eds., Quark Matter '88, Proc. Sixth Int. Conf. on Ultrarelativistic Nucleus-nucleus Collisions, Nucl. Phys. **A498**(1989).

[2] S. Gavin and R. Vogt, preprint LBL-27417.

[3] B. Andersson et al, Phys.Rep. **97**(1983) 31; B. Andersson, G. Gustafson and B. Nilsson-Almqvist, Nucl.Phys.**B281**(1987) 289

[4] M. Gyulassy, Proc. Eighth Balaton Conf. on Nucl. Phys., (ed. Z. Fodor, KFKI, Budapest 1987); CERN preprint CERN-TH.4794/87 (1987).

[5] A. Cappela et al, Z. Phys. **C3**(1980) 68; **C33**(1987) 541; J. Ranft, Phys. Lett. **B187**(1987) 379.

[6] K. Werner, Phys. Rev. Lett. **62**(1989) 2460.

[7] H. Heiselberg, NORDITA preprint 89/32 N.

[8] J. Ftáčnik, P. Lichard, and J. Pišút, Phys. Lett. **207B**(1988) 194; S. Gavin, M. Gyulassy, and A. Jackson, Phys. Lett. **208B**(1988) 257; R. Vogt, M. Prakash, P. Koch, and T. H. Hansson, Phys. Lett. **208B**(1988) 263; J.-P. Blaizot and J.-Y. Ollitrault, Phys. Rev. **D39**(1989) 232.

[9] M. Gyulassy and S.S. Padula, Phys. Lett. **270B**(1989) 181.

[10] M. Gyulassy and M. Plümer, preprint LBL-27605.

[11] U. Heinz, P.R. Subramanian, H. Stöcker, and W. Greiner, J. Phys. G: Nucl. Phys. **12**(1986) 1237; P. Koch, B. Müller, H. Stöcker, and W. Greiner, Mod. Phys. Lett. **A8**(1988) 737.

[12] J. Knoll, Z. Phys. **C38**(1988) 187.

[13] B. Jacak, NA34 collab., private communication; J. Costales, E802 collab., private communication.

[14] J. D. Bjorken, Phys. Rev. **D27**(1983) 140.

[15] V. Flamino *et al.*, CERN-HERA Report 84-01, 1984.

[16] C. M. Ko and X. Ge, Phys. Lett. **B205**(1988) 195; C. M. Ko and L. H. Xia, Phys. Rev. **C40**(1989) R1118.

[17] P. Koch and C. B. Dover, Phys. Rev. **C40**(1989) 145.

[18] A. Bialas and M. Gyulassy, Nucl.Phys. **B291**(1987) 793

[19] K. Werner, Phys. Lett. **B219**(1989) 111.

$\sqrt{s}$ (AGeV)	10	20	20	200
$A+B$	Au+Au	S+Au	Au+Au	Au+Au
$d\overline{N}/dy\|_{t_0}$	14	7	23	40
$dN/dy\|_{t_0}$	93	11	48	40
dN_ρ/dy	90	31	106	132
$d\overline{N}/dy\|_{t_F}$	0.3–0.7	2.9–3.1	4–5	11–13
$dN/dy\|_{t_F}$	79–80	6.9–7.1	29–30	11–13
t_F/t_0	6	3.3	6	12

Table 1.
Calculated initial and final rapidity densities at $y = 0$ for the value of t_F/t_0 indicated. The rapidity densities of baryons include p, n, Λ etc.

rapidity densities, dN/dy and $d\overline{N}/dy$, in Table 1 include all baryonic species — as opposed to Fig. 2, where the $\overline{p}$ distributions are presented).

Alternatively, we can extract information on the initial rapidity densities from data, provided that we know t_F/t_0 from a dynamical model or from other experiments. For the reaction Au+Au, Fig. 3 illustrates how such information can be obtained from the correlation between the measured antiproton yield and the proton contribution to the baryonic-charge rapidity density. The curves correspond to fixed values of the *initial* scalar baryon rapidity density, $dN_S/dy \equiv dN/dy + d\overline{N}/dy$, a quantity which reflects the degree of excitation of the system. The correlation is essentially independent of the beam energy and varies slowly with the projectile and target type through the derived dependence on t_F/t_0 (cf. eqs.(1), (9)). The expected correlations for the initial conditions taken from Fig. 1 are shown in Fig. 3 as "data" points. A complex behavior of the scalar density expected from LUND for increasing energy is revealed — we see that the initial dN_S/dy is relatively high at the lowest energy simply because the density of baryons is high due to stopping. The scalar density drops as transparency becomes more pronounced (cf. Fig. 1) but rises again at RHIC due to the enhanced production of baryon-antibaryon pairs.

The full hadrochemistry problem involves back reaction processes that could produce antibaryons through a variety of reactions in a high density hadron gas, $\pi\pi \to N\overline{N}$, $\rho\rho \to N\overline{N}$, etc. We expect that the contribution of these channels to antibaryon production will be small, however, since the channels that involve the most abundant mesons are endothermic — the π, K, η, ρ, ω, K^* and η' which constitute $\sim 90\%$ of the secondaries in LUND have masses of less than 1 GeV so that the reactions are threshold suppressed. To illustrate the effect of possible inverse processes on the yield, we take the $\rho\rho$ channel to be dominant. For nuclear collisions at Bevalac energies, Ko and Ge [16] pointed out that the $\rho\rho$ channel can be strong, since the ρ is massive and $p\overline{p} \to \rho\rho$ has a relatively large branching ratio – they estimate $\sim 5\%$. Moreover, ρ's are plentiful at CERN energies, accounting for $\sim 20\%$ of the secondaries. We add the source term $\langle\sigma_s v\rangle {n_\rho}^2$ to (4), where n_ρ is the ρ density. Applying detailed balance to $p\overline{p}$ annihilation data as in Ref.[16], we find that $\langle\sigma_s v\rangle \approx \langle\sigma_{\rho^+\rho^-} v\rangle \approx 0.2\,\mathrm{mb}$ for an effective temperature $T_\rho \approx 160$ MeV, as characterizes the transverse momentum distribution in LUND. To obtain the upper bounds for the final rapidity densities of baryons and antibaryons in Table 1, we assumed that dN_ρ/dy is time-independent and given by the values shown in Fig. 1 . The modified rate equation then determines the upper bounds in Table 1; the lower bounds correspond to the absence of a ρ contribution. The conserved-ρ approximation overestimates the effect of antibaryon regeneration by overemphasizing the effect of the strongest channel, since ρ decay is neglected.

Finally, we briefly comment on antibaryon production at AGS energies. At these energies we expect the nuclei to be fully stopped (see Fig. 1), so that Landau hydrodynamics may be more appropriate than our scaling approximation. Furthermore, our simplified treatment of freezeout is not applicable because t_F is on the order of the spread in the formation time t_0 and a much more detailed dynamical

Figure Captions

Fig. 1 Rapidity distributions of baryons, antibaryons and ρ mesons in the absence of final-state interactions, calculated for Au+Au.

Fig. 2 Final rapidity distribution of antiprotons in 200 AGeV S+Au and Au+Au for $t_F(\mathrm{S}+\mathrm{Au}) \sim 5$ fm and $t_F(\mathrm{Au}+\mathrm{Au}) \sim 12$ fm and various t_0.

Fig. 3 Correlation of the final rapidity densities of antiprotons and of the proton contribution to the baryonic-charge, for various assumed *initial* scalar baryon rapidity densities dN_S/dy (baryons + antibaryons). The calculated "data" points are from table 1.

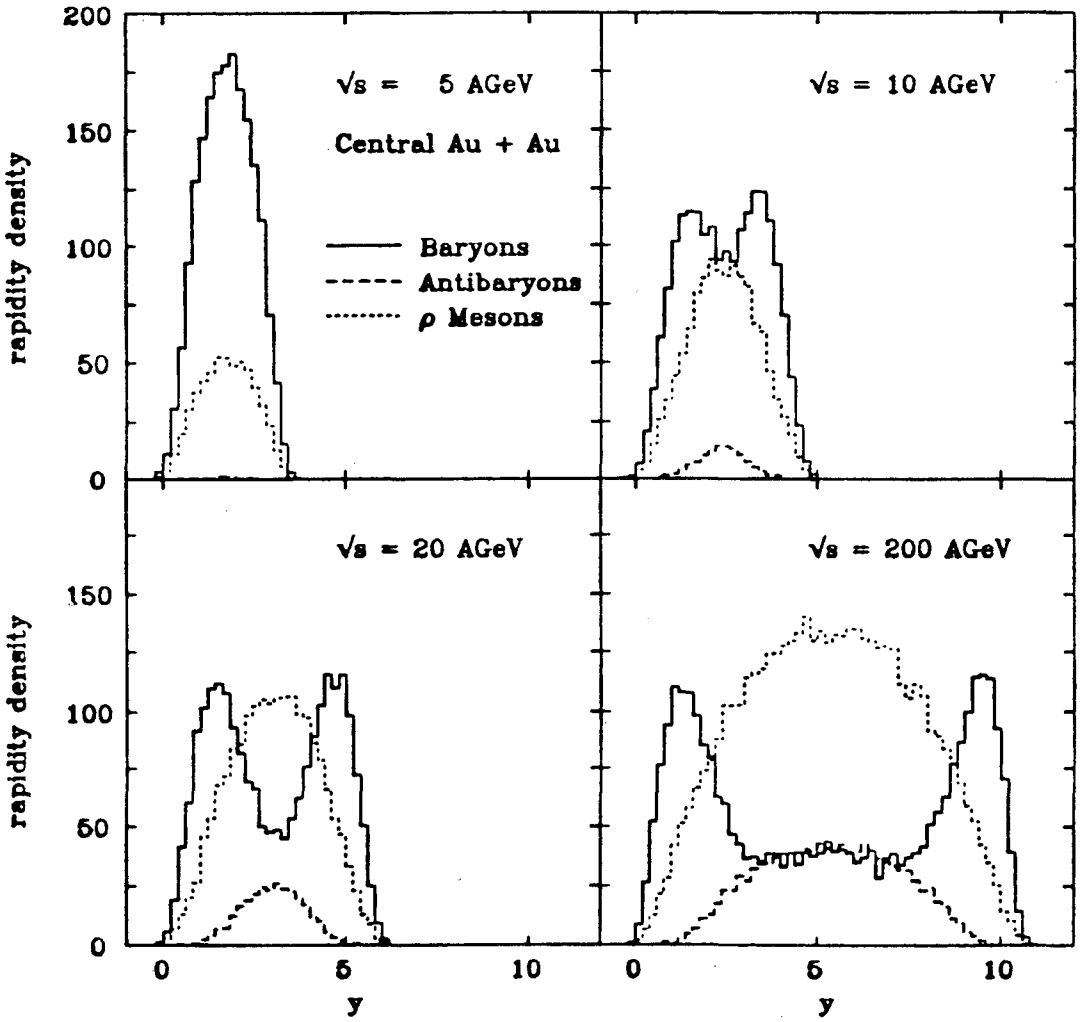
√s = 5 AGeV
Central Au + Au
Baryons
Antibaryons
ρ Mesons
√s = 10 AGeV
√s = 20 AGeV
√s = 200 AGeV
rapidity density
rapidity density
y
y
0
50
100
150
200
0
5
10

Fig. 1

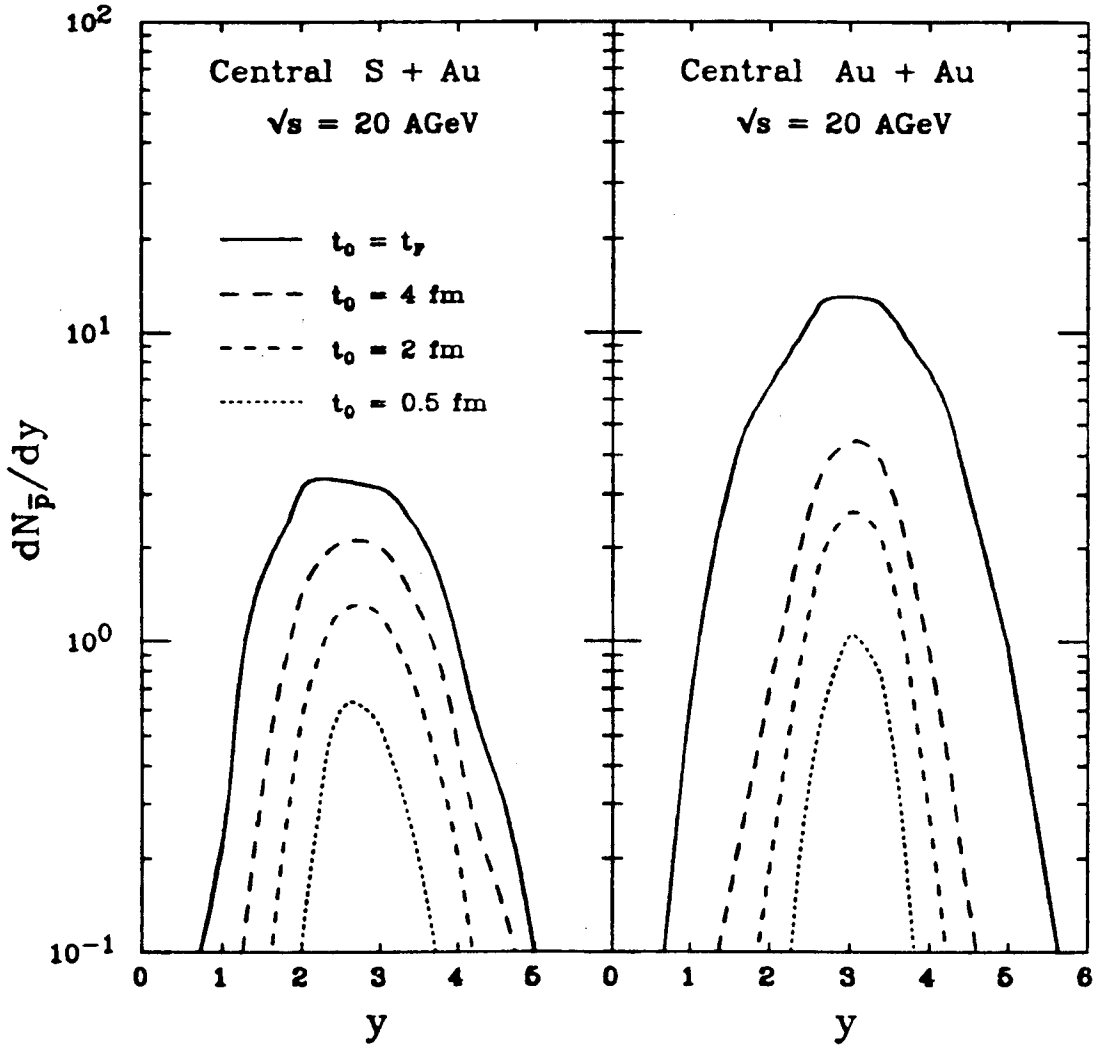
Central S + Au
√s = 20 AGeV
Central Au + Au
√s = 20 AGeV
$t_0 = t_f$
t_0 = 4 fm
t_0 = 2 fm
t_0 = 0.5 fm
$dN_{\bar{p}}/dy$
10^2
10^1
10^0
10^{-1}
0 1 2 3 4 5
0 1 2 3 4 5 6
y
y

Fig. 2

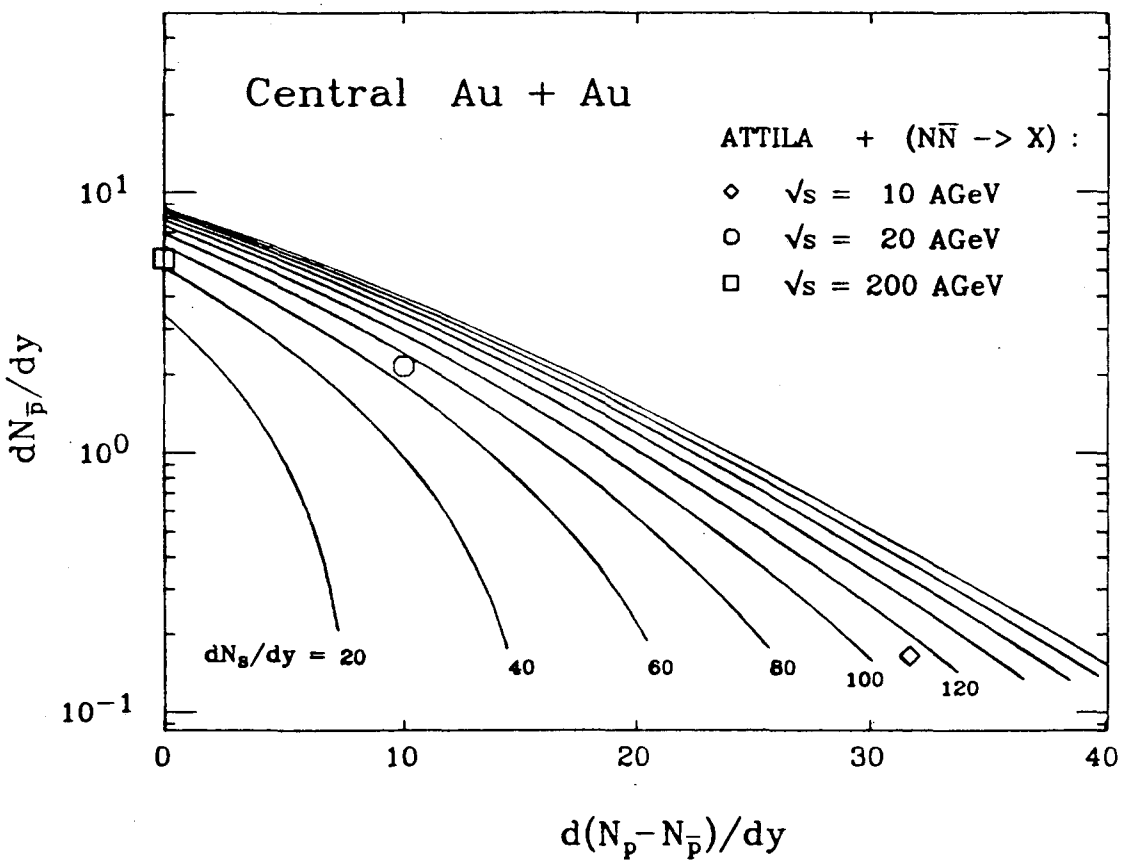
Central Au + Au
ATTILA + (N$\bar{N}$ -> X) :
◇ √s = 10 AGeV
○ √s = 20 AGeV
□ √s = 200 AGeV
10^1
10^0
10^{-1}
$dN_{\bar{p}}/dy$
dN_B/dy = 20
40
60
80
100
120
0
10
20
30
40
$d(N_p - N_{\bar{p}})/dy$

Fig. 3

LAWRENCE BERKELEY LABORATORY
TECHNICAL INFORMATION DEPARTMENT
1 CYCLOTRON ROAD
BERKELEY, CALIFORNIA 94720